Supporting Information

Bouchard et al. 10.1073/pnas.0813019106

SI Text

MRI Contrast Sensitivity. It is instructive to examine possible reasons for the superior MRI contrast enhancement. Larger (micron-size) superparamagnetic particles can be manufactured by embedding nanoparticles into a polymer matrix. It is unclear; however, that the net moment would be expected to increase linearly with the size of the construct as due to the misalignment of the multiple magnetic domains, some amount of cancellation will take place, leading to a smaller net magnetic moment per unit volume and also per particle. This is true even in the presence of a strong magnetic field as used in MRI, because the anisotropy energy of the material which causes the random reorientation of single domains is typically much larger than the Zeeman energy. When comparing our Co nanowonton to conventional small paramagnetic iron oxide (SPIO) particles under an applied field that saturates the magnetization (including any hysteresis effect), the relevant quantity for molecular imaging purposes, where a binding event involves one ligand moiety per target molecule, is the per-particle relaxivity. In a homogeneous solution of ferromagnetic particles, the per-particle relaxivity for water is proportional to the square of the magnetic moment of relaxing centers. The saturation magnetization of fcc-Co is 3.42 times higher than magnetite (Fe_3O_4) (1), which implies a per-particle relaxivity that is nearly 12 times larger than magnetite. This has important implications for T_2-weighted MRI, which depends exponentially on the relaxation rate. For example, a 1 μM concentration of Co nanowonton particles with T_2 relaxivity of 1×10^7 $s^{-1}{\cdot}mM^{-1}$ (as measured experimentally for our nanowonton) and an echo time of 50 ms produces an exponential decay factor that is 100 times larger than for magnetite. This is how substantial improvements in NMR signal changes can be obtained for the same particle size. Regarding our actual numbers, the measured T_2 relaxivity is 1×10^7 $s^{-1}{\cdot}mM^{-1}$, which is a 5-orders-of-magnitude higher "per-particle" relaxivity than the monocrystalline iron oxide nanoparticles (MION) of ref. 2, in which a rather low 121 $ms^{-1}{\cdot}M^{-1}$ was obtained. Our particles are also bigger than Lu's (2) (60 nm average diameter, vs. 18 nm). This larger particle diameter adds a factor of 37 to the magnetic moment per particle, or 3 orders of magnitude to the relaxivity. These 2 effects (choice of material, particle diameter) add up to 5 orders of magnitude, which explain the difference between our results and Lu's results (2) on iron oxide. In figure 9 of Lu's paper, we can see that they require 10^{-4} M concentrations to observe an effect in the T_2-weighted contrast in phantoms. Our particles can be readily seen at 2.5×10^{-12} M in MRI images. This is a >7 orders of magnitude difference; this number includes the exponential effects of T_2-weighted contrast mentioned above. Cho et al. (3) report better results on Fe/Au nanoparticles, as would be expected for iron based on its high saturation magnetization, but they only report detectability thresholds of 300 pM in phantoms. (One could argue that the 300 pM cannot be seen in their figure 4, and the number is probably more like 600 pM. Also note that they report metal concentrations. The numbers we quote are converted to particle concentrations for comparison.) This number falls short of our cobalt nanoparticles detectability threshold. Their reported T_2 relaxivity, when converting the number 28.15 $mM^{-1}{\cdot}s^{-1}$ from their Table 1 to per-particle relaxivity (using 1 mM = 6 nM for iron particles of 18-nm diameter), we get $\approx 4 \times 10^6$ $mM^{-1}{\cdot}s^{-1}$, slightly lower than ours. Because fcc-Fe has a higher saturation magnetization, there is potential for even higher particle relaxivity than cobalt by further increasing the particle diameter, but this is not demonstrated in their paper.

In Vivo Toxicity and Stability. Au nanoparticles are widely used in EM studies for live cells and no observable toxicity has been detected up to nM concentrations. Of all of the metal coatings examined so far, Au coatings have shown the lowest levels of toxicity. In animal studies, Au nanoparticles such as nanoshells have shown good dose tolerance. See refs. 4, 5, and 6 for relevant studies that establish the in vivo nontoxicity of Au particles. In dose-dependent studies, we have demonstrated (see Fig. S3) that up to micromolar concentration, Au nanoparticles induce no elevated apoptosis in cells.

Extension to Other Modalities. As shown in Fig. S4, there are situations where complementary information is crucial, as it is easy to find situations where single modality imaging will be insufficient. We believe that the combined PAT/MRI is extremely powerful for diagnostic imaging. MRI provides volume information whereas PAT provides edge detection. Our particles could certainly be used with position emission tomography (PET), using Au-coated radioactive cobalt, e.g., ^{60}Co, and CT; although both of these modalities are beyond the scope of this article. PAT, although in relative infancy compared to PET and CT, has the exciting possibility of providing edge-detection contrast, which is a definite advantage over MRI, and other imaging modalities.

PAT Imaging of Rat Tail Joints. CD hairless rats (≈300 g; Charles River Laboratory) were included in this study. Whole tails were harvested from the rat bodies shortly after the rats were killed. An electrocautery device (SurgiStat; Valleylab) was then used to clot blood and seal vessels. Each rat tail was placed in the PAT system along the *Z*-axis as shown in Fig. S1. The first proximal segment of the rat tail was fixed on a rotational stage that, driven by a stepper motor, could rotate the tail around its axis. The imaged joint was about 2.5 cm from the rat trunk, where the diameter of the tail joint was 8–9 mm. First, a PAT image of a rat tail joint was taken before the administration of the contrast agent. After that, 0.05 mL of agent with a concentration of 100 pM was injected intraarticularly along the direction indicated by the arrows in Fig. S4*B*. Then another PAT image of the same joint was taken. The total numbers of nanowonton particles introduced into the regional joint tissue were on the order of 10^9 (i.e., femtomole). All of the experimental parameters for the images taken before and after the administration were kept the same, except that the sample might be moved slightly during the administration of contrast agent.

Cross-sectional imaging of the rat tail joint with and without injection of the nanowonton contrast agent (0.05 ml, 100 pM) are compared in Fig. S4 *A* and *B*. Following the administration of contrast agent, which perfused the front part of the joint space, hyperintensities are readily observed in the periosteum (Fig. S4*B*). With a comparatively limited detection bandwidth, the current PAT system is more sensitive to the edges of an absorbing object (arrow in Fig. S4*B*). Although the sensitivity of this PAT system to nanowonton contrast agent can be improved further by employing a laser source with better energy stability and a more sensitive transducer(s), this level of detection sensitivity is similar to or even higher than pure optical imaging for metallic particles (to). The general tendency of PAT to perform edge detection is evident when high frequency ultra-

sound detection is used. PAT with deeper penetration depth can be achieved by using laser light in the near infrared region, capitalizing on the ability to tune the absorption profile of the nanoparticles or the thin film coatings (Fig. S2). An anatomical section of the same tail joint is presented in Fig. S4*C*.

1. Hutten A, et al. (2004) New magnetic nanoparticles for biotechnology. *J Biotechnol* 112:47–63.
2. Lu J, et al. (2006) Solid-state synthesis of monocrystalline iron oxide nanoparticle based ferrofluid suitable for magnetic resonance imaging contrast application. *Nanotechnology* 17:5812–5820.
3. Cho SJ, Jarrett BR, Louie AY, Kauzlarich SM (2006) Gold-coated iron nanoparticles: a novel magnetic resonance agent for T_1 and T_2 weighted imaging. *Nanotechnology* 17:640–644.
4. Liao H, Nehl CL, Hafner JH (2006) Biomedical applications of plasmon resonant metal nanoparticles. *Nanomedicine* 1:201–208.
5. Cai Q, et al. (2007) Colloidal gold nanoparticles as a blood-pool contrast agent for X-ray computed tomography in mice. *Invest Radiol* 42:797–806.
6. Kim D, Park S, Lee JH, Jeong W, Jon S (2007) Antibiofouling polymer-coated gold nanoparticles as a contrast agent for in vivo X-ray computed tomography imaging. *J Am Chem Soc* 129:7661–7665.
7. Liu GL, et al. (2006) A nanoplasmonic molecular ruler for measuring nuclease activity and DNA footprinting. *Nat Nanotechnol* 1:47–52.
8. Loo C, et al. (2004) Nanoshell-enabled photonics-based imaging and therapy of cancer. *Technol Cancer Res T* 3:33–40.

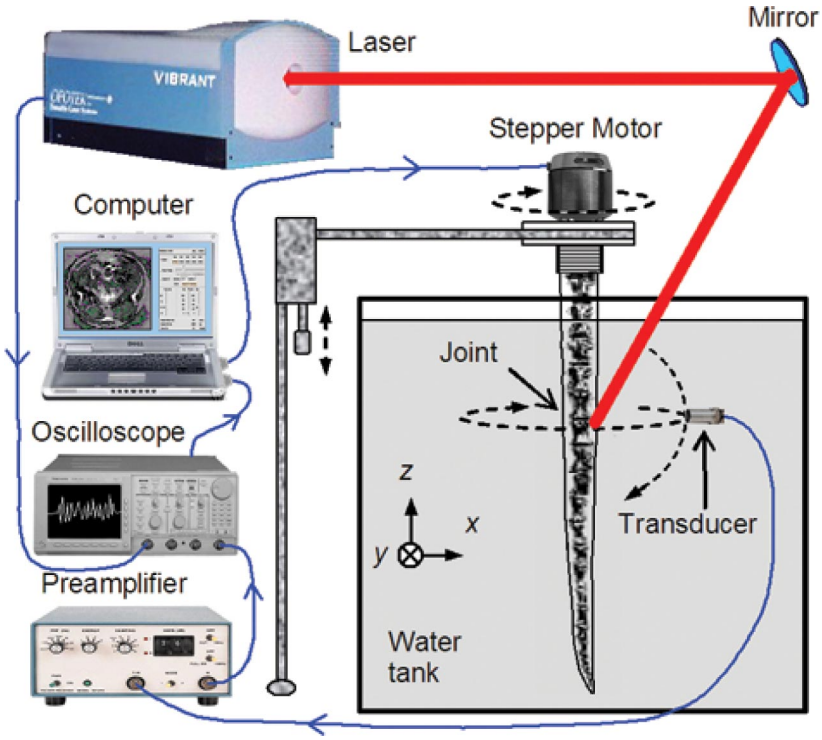

Fig. S1. Schematic of the PAT system.

Fig. S2. Schematic of Chinese wonton.

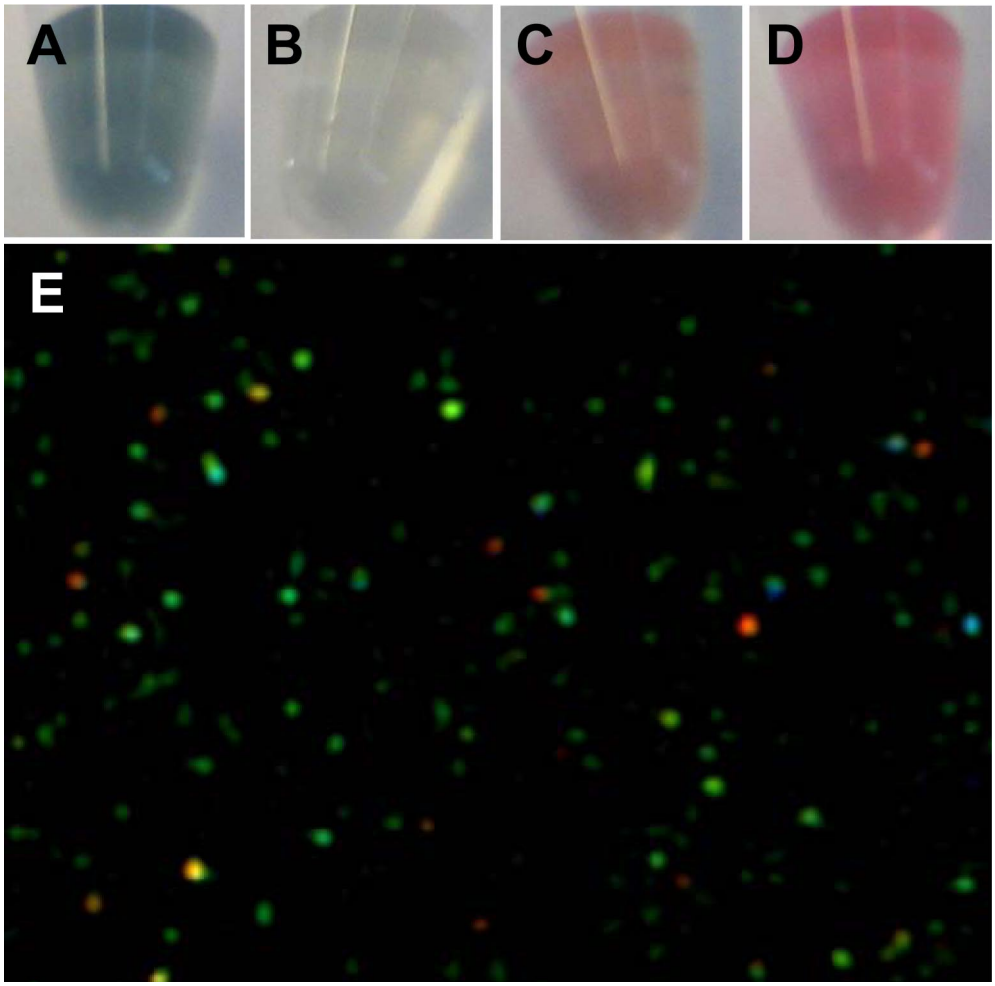

Fig. S3. Tunability of scattering wavelength of nanowonton by changing the size of the nanowonton. (*A*) The nanowonton with exterior diameter of 60 nm used in the study. (*B*) 80 nm diameter nanowonton. (*C*) 40 nm nanowonton. (*D*) A 10 nm nanowonton. (*E*) Scattering light microscopy image of the 60 nm diameter nanowonton with 700 nm peak scattering wavelength used in the study.

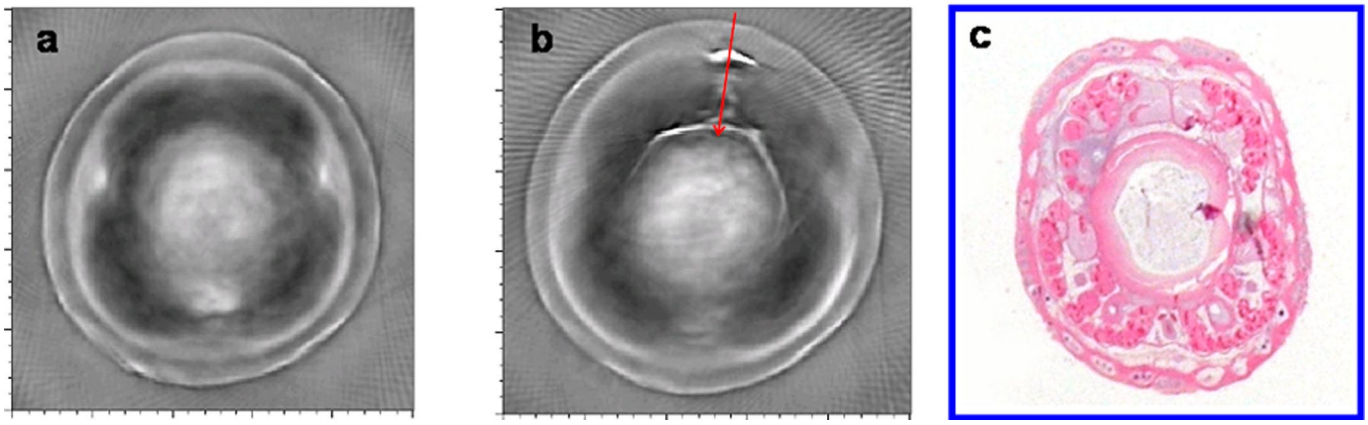

Fig. S4. Photoacoustic imaging of rat tail joint taken (*a*) before and (*b*) after the administration of nanowonton contrast agent at 100 pM. For comparison purpose, we also have obtained the (*c*) histological photograph of a similar cross section showing the periosteum. In *a* and *b*, grayscale is in arbitrary units of relative optical absorption, and *xy* scales are 1 cm × 1 cm.

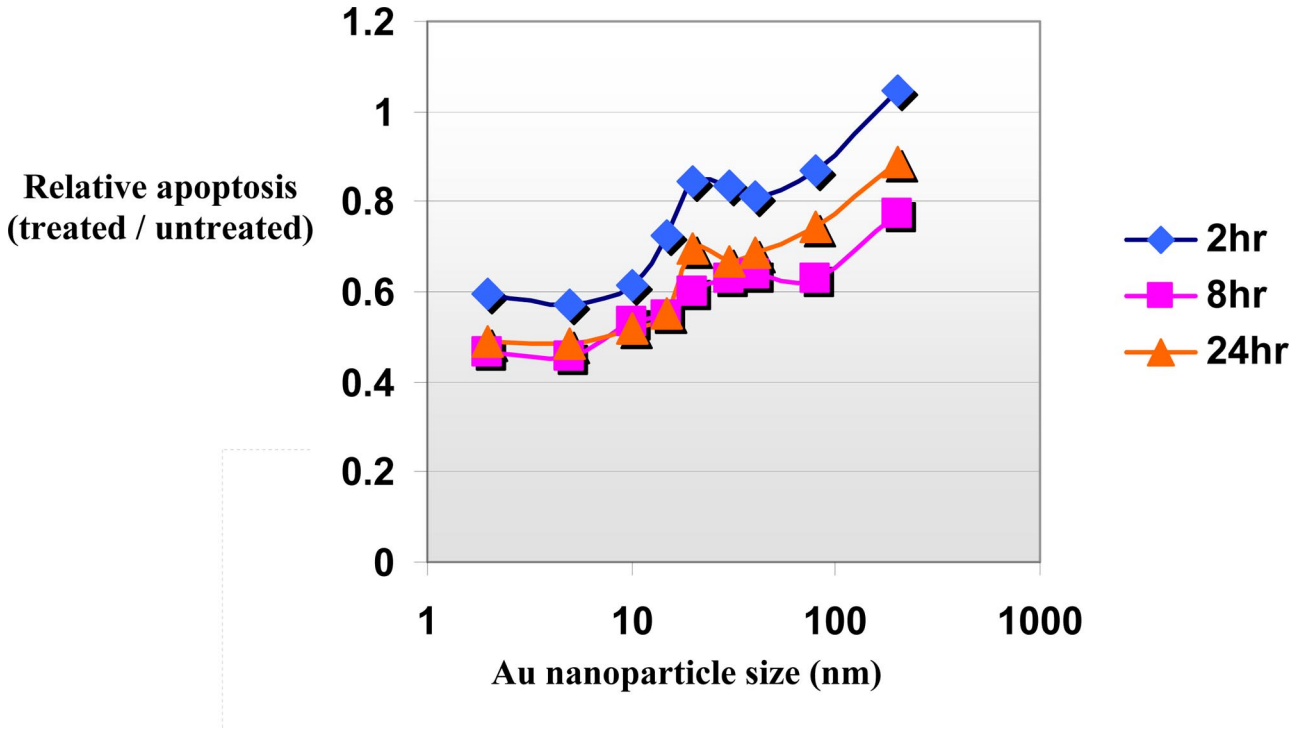

Fig. S5. Au nanoparticles ranging from 2 to 200 nm are used to treat a model cell system (Jurkat cells) at 1.2 mg/L final concentration. Less than 1.2% of total cells show apoptosis. Result shows no significant difference from untreated cells, which have an apoptosis rate of 1%. The results show absence of toxicity with Au nanoparticles in the same size range.